Guides for Authors

TYPING: All manuscripts must be in English, typed double-space on one side of the page throughout (including footnotes, references, tables, legends) on 8.5" x 11" or A4 white paper leaving at least 1 inch left hand margin.

INTRODUCTORY MATERIAL: The first page of the manuscript should have a concise title limited to about 15 words and the names of all authors, complete mailing address for correspondence, telephone, fax numbers and email address. Please indicate with an asterisk (*) the author to whom correspondence regarding the manuscript should be directed.

ABSTRACT: All manuscripts must contain an informative 150 to 300 words abstract explaining the essential contents of the work, key ideas and results.

FIGURES: It is very important to supply high quality figures in a form suitable for reproduction. All figures, tables, illustrations, photographs should be prepared in such a way that they could be printed in a single column size with a width of 3 1/4 inches or 8.25 cm. Use 14 ARIAL BOLD font for legends and 12 ARIAL font for numbering/wordings in figures, use the same font for all figures. Only if absolutely necessary should figures/tables/photos occupy double columns. Each figure must be referred to in the text and will be printed in black and white unless otherwise instructed by the authors. Each Figure should be submitted on a separate sheet and marked with the name of the author, title of manuscript and figure number. All formulae and figures should be carefully drafted and never drawn freehand. High quality original figures and glossy prints of all photographs are required. Photocopies of the figures and photographs are not acceptable.

PHOTOGRAPHS: Half-tone illustrations should be supplied as clear, glossy, unmounted prints. The author's name, title of manuscript and figure number should be written on the back.

TABLES: Each table must be referred to in the text. Each table should be typed double-spaced on a separate sheet and identified sequentially by Arabic numerals corresponding to the order in which they appear in the text. Each table should have a brief explanatory title, which should be labeled unambiguously. The position of each table should be clearly marked in the text.

UNITS: Internationally accepted units of measurement must be used. The units of measurement are used in conjunction with their numerical values; the units should be abbreviated as suggested below. If more commonly used units are adopted, conversion factors should be given at their first occurrence. Greek symbols may be

used.

%, ℃, nm, μm (not m), mm, cm, cm3, m, h (or hr), min, s (or sec), μg, mg, g (or gm), kg, cal, kcal, in. (or write out inch), ml [write out liter(s)].

The APS style guide can be used as a general reference on matter of units, grammar and formatting.

ABBREVIATIONS: No abbreviations are allowed in the title and abstract and should be defined the first time they are used within the text. The "Journal of Nanoscience and Nanotechnology" should be abbreviated as J. Nanosci. Nanotechnol. for the citation purpose.

REFERENCES: References should be in the proper format on a separate page, numbered in the sequence in which they occur in the text. Cite references numerically as superscripts in the text and list at the end of the manuscript. References should be listed in the following style:

1. H. R. Jones and M. K. Wiles, J. Phys. Chem. 78, 8356 (1999)
2. J. M. Cowley, Diffraction Physics, Elsevier, Amsterdam (1995)
3. C. E. Krill, R. Harberkorn and R. Birringer, in Handbook of Nanostructured Materials and Nanotechnology edited H. S. Nalwa, Academic Press, San Diego (1999), Vol. 2, p.155.
4. J. P. Turner and P. C. Chu, in Microelectronics, T. J. Kern, Ed., Materials Research Society, Warrendale, PA (1995), Vol. 143, p.375.

Do not use the phrases "et al." and "ibid." in the reference section. Instead, the names of all authors in a reference must be listed.

ACKNOWLEDGEMENTS: These should be brief and placed at the end of the text before the references.

PROOFS: Page proofs for the correction of printer's errors only will be dispatched to the corresponding author denoted with an asterik (*) unless otherwise requested. Alterations at this stage are not allowed as they are expensive and may have to be charged to the authors. The proofread copy and reprint order form must be returned within 72 hours.

WARRANTIES AND COPYRIGHTS: By submitting the manuscript, the authors warrant that the entire work is original and unpublished; it is submitted only to this Journal and all text, data, figures/tables or other illustrations included in the research article are completely original and unpublished, and these have not been previously published or submitted elsewhere in any form or media whatsoever. All authors are responsible for the complete contents of their manuscript. The author(s) warrant that

the work contains no unlawful or libelous statements and opinions and liable materials of any kind whatsoever, do not infringe on any copyrights, intellectual property rights, personal rights or rights of any kind of others, and does not contains any plagiarized, fraudulent, improperly attributed materials, instructions, procedures, information or ideas that might cause any harm, damage, injury, losses or costs of any kind to person or property. Each author(s) agrees to defend, indemnify, and hold harmless American Scientific Publishers and the Editors for any breach of such warranties. It is authors' responsibility to obtain written copyright permissions from other sources (publishers) for reproduction of any figures, tables, photos, illustrations, text or other copyright materials from previously published work. It is the policy of American Scientific Publishers to own the copyright of all contributions it publishes. To comply with the U.S. Copyright Law, a Copyright Transfer Form that transfer copyright of the article to the publisher must be completed by the authors prior to publication of an accepted article in this journal. Authors must submit a signed copy of the Copyright Transfer Agreement with their manuscript.

ABSTRACTING AND INDEXING: American Scientific Publishers has no control whatsoever over abstracting and indexing of their scientific journals in any types of databases (SCIE, Scopus, Compendex, PubMed, CPCI, etc.), therefore, the publisher does not guarantee and take any responsibilities whatsoever for any kind of abstracting and indexing coverage of the published work in any types of databases whatsoever.

Date of Submission:
Date of Acceptance:

Template

Polarity Reversion of the Operation Mode of HfO_2-Based Resistive Random Access Memory Devices by Inserting Hf Metal Layer

Ching-Shiang Peng,[a,z] Wen-Yuan Chang,[b,z] Ming-Ho Lin,[a] Wei-Su Chen,[c] Frederick Chen,[c] and Ming-Jinn Tsai[c,*]

aDepartment of Materials Science and Engineering, National Tsing-Hua University, Hsinchu 300, Taiwan ROC

bInstitute of Photonics and Optoelectronics, National Taiwan University, Taipei 106, Taiwan

cElectronics and Optoelectronics Research Laboratory, Industrial Technology Research Institute, Chutung, Hsinchu 310, Taiwan

* Corresponding author: ming.j.tsai@mail.com.cn

The reversion of polarity within bipolar resistive switching operation occurs in Pt/HfO_2/TiN and Pt/Hf/HfO_2/TiN resistive random access memory devices. This reversion of voltage polarity is the result of interface generation which induces a conduction mechanism transformation from Poole-Frenkel emission to space charge limited current mechanism. To prove the reversion of polarity, this study uses curve fitting of I-V relations to verify the conduction mechanism theoretically and physical analysis to verify the oxygen ion distribution practically. The proposed Pt/Hf/HfO_2/TiN devices exhibit good resistive switching characteristics, such as good uniformity, low voltage operation, robust endurance (10^3 dc sweep), and long retention (3×10^4 s at 85 ^oC).

Keywords: HfO_2, Resistive random access memory, Hf Metal Layer

1. Introduction

Resistive random access memory (RRAM) is an ideal candidate for non-volatile memory applications because of its simple structure, great scalability, fast switching speed, low power consumption, and compatibility with complementary metal-oxide semiconductor technology.[1,2] RRAM devices achieve the memory effect using the switchable resistance transformation between a high resistance state (HRS) and a low resistance state (LRS), and typically consist of a metal/insulator/metal structure. RRAM devices generally have two switching modes (unipolar and bipolar), which alternate based on the operating voltage polarity. Unipolar resistive switching occurs in any single voltage bias and does not depend on voltage polarity. Conversely, bipolar resistive switching depends on the variation of voltage polarity to complete the set (i.e., from the HRS to the LRS) and reset (i.e., from the LRS to the HRS) processes. Recent developments in RRAM have shifted to bipolar RRAM for several advantages, including a stable ON/OFF ratio, robust endurance, good retention, smaller switching voltage fluctuation, and the one selector-one resistor (1S1R) application.[3] The transition metal oxide, HfO_2, is already widely used in semiconductor industries because of its superior physical properties, such as large permittivity, subsequent band gap, and excellent thermal stability.[4] In addition to its use as high-k/metal gate stacks, HfO_2-based RRAM has attracted significant attention for its potential in next-generation nonvolatile memory. HfO_2-based RRAM devices are formed by an electric-field induced conductive filaments formation/rupture process, and possess superior bipolar resistive switching for future RRAM applications.

The localized filamentary conducting paths in the thin films are diverse in each switching, leading to the nonuniform distributions of switching voltages and resistance states, which result in irresolvable errors in the RRAM operations. Thus, how to effectively improve the stability of switching behavior is an essential issue for practical application of the RRAM. Researchers have used many methods to improve resistive switching characteristics and change thin-film properties, such as embedding nanocrystals,[5] doping effects,[6,7] and embedding metal layer.[8-11] The embedding metal layer method typically serves as an interfacial oxygen storage layer, leading to oxygen ion concentration variation and diffusion. This in turn confines the conductive filament formation and rupturing within insulators and improves the uniformity of resistive switching characteristics. The interfacial layer also play a key role in polarity effect and resistive switching, and is dominant in the conversion of polarity from unipolar resistive switching to bipolar resistive switching, as shown by Yoo *et al.*[12] The reversion of polarity within bipolar resistive switching operation in Pt/HfO_2/TiN and Pt/Hf/HfO_2/TiN devices was observed in this work. The polarity reversion may be significantly affected by interfacial layer generation, inducing the change of conduction mechanisms in two device structures. The I-V relation and physical analysis in this study both provide proofs of the reversion of polarity. Pt/Hf/HfO_2/TiN RRAM devices also exhibit good resistive switching characteristics by inserting Hf metal layer resulted in the production of HfO_x layer as an oxygen storage layer.

2. Experimental Details

In this study, RRAM devices consist of Pt/HfO_2/TiN and Pt/Hf/HfO_2/TiN structures. HfO_2 thin films were deposited on TiN (50 nm)/Ti (150 nm)/SiO_2 (200 nm)/p-Si substrates at 200 ^oC using the atomic layer deposition (ALD) method. The HfO_2 thin film (derived from TEMAH and H_2O precursors) was controlled at approximately 10 nm, and the deposition thickness of HfO_2 per ALD cycle was approximately 0.1 nm. After HfO_2 thin-film deposition, Hf and Pt metal layers measuring 40 nm and 70 nm in thickness were capped continuously by dc sputtering and patterned by a shadow mask with a diameter of 200 μm. The Pt capping layer prevents oxygen penetration from the atmosphere. The Pt/Hf/HfO_2/TiN device was subjected to post metal annealing (PMA) at 400 ^oC for 30 s in a N_2 atmosphere. For a comparison, a reference sample made without Hf layer and PMA process was also prepared, denoted as Pt/HfO_2/TiN device. The chemical-bonding states of Hf atoms in thin films were analyzed using the X-ray photoelectron emission spectrum (XPS). The electrical properties of the devices were measured using a Keithley 4200 semiconductor parameter analyzer. During the voltage-sweeping mode measurement, the bias was defined as positive when the current flowed from the top electrode to the bottom electrode, and was defined as negative when the current flowed in the opposite direction.

3. Results and Discussion

Figures 1a and 1b show the reverse polarity operation within bipolar resistive switching. Figure 1a shows that the set operation by a negative bias and the reset operation by a positive bias appear in the electrical characteristics of Pt/HfO_2/TiN RRAM devices. The same polarity was observed in similar devices described in

previous researches.[13,14] After the Hf metal layer deposition and PMA processes, Pt/Hf/HfO_2/TiN RRAM devices show reverse polarity operation (i.e., the set operation by a positive bias, and the reset operation by a negative bias) in a stable resistive switching situation, as shown in Fig. 1b. The experimental results and literatures review in this study will confirm that the reverse polarity is correlated with interface-producing and conduction mechanism, transforming between two structures. In Pt/HfO_2/TiN RRAM devices, the conduction mechanism in pure HfO_2 thin films is usually attributed to the Poole-Frenkel emission.[15,16] The Poole-Frenkel emission equation can be expressed as $J = (qN_c\mu)E\exp\left(-\frac{q\Phi t}{kT} + \frac{q\sqrt{\frac{qE}{\pi\varepsilon_\gamma\varepsilon_0}}}{rkT}\right)$, in which q is the electronic charge, N_c is the density of states in the conduction band, μ is the electronic drift mobility, $q\Phi$t is the trap level below the conduction band, ε_γ is the dynamic dielectric constant, ε_o is the permittivity of free space, k is Boltzmann's constant, T is the temperature, and r is a coefficient ranging between 1 and 2.[17,18] If r = 2, the conduction mechanism is so-called the normal Poole-Frenkel emission. However, when the insulator contains another influential trap, r is equal to 1 and the conduction is called the modified Poole-Frenkel emission. In the reset process, the $\ln\left(\frac{J}{E}\right) - \sqrt{E}$ relationship of the HRS in the high electric field exhibits linear dependence, as shown in Fig. 2a. Accordingly, a refractive index of n = 2.05 can be obtained from the slope of the Poole-Frenkel plot at r = 1. This value is close to that of HfO_2 thin films reported in previous studies.[19,20] The consistency between these results and fitting data implies that Poole-Frenkel emission is the primary conduction mechanism in Pt/HfO_2/TiN RRAM devices.

Voltage polarity during resistive switching operation in the Pt/HfO_2/TiN RRAM device can be reversed by Hf metal deposition and the PMA process. This study applies theoretical deduction and physical analysis to investigate the reason for this polarity reversion. Initially, curve fitting was executed for the negative bias region of I-V characteristics in the Pt/Hf/HfO_2/TiN RRAM device. Figure 2b shows the resulting double-logarithmic plots. In the reset operation, Child's square law ($I \sim V^2$) is obeyed in the high-voltage bias by slope ~ 2 in the HRS, whereas Ohm's law ($I \sim V$) is obeyed in the low-voltage bias by slope ~ 1 in the HRS. According to the fitting results, the conduction mechanism of the proposed Pt/Hf/HfO_2/TiN RRAM devices is caused by space charge limited current (SCLC) mechanism.[9,16,21] Many studies have indicated that the SCLC mechanism is related to the insulating interfacial layer formation between metal layers and oxide thin films. This suggests the presence of an oxide interfacial layer between the Hf metal and the HfO_2 thin film, which might be partial oxide HfO_x ($x<2$).[9,16,21] After the PMA process, many oxygen ions may diffuse from the HfO_2 thin film to the Hf metal, resulting in the formation of HfO_x with oxygen deficiencies and Hf oxidation. To verify upon deductions of Pt/HfO_2/TiN and Pt/Hf/HfO_2/TiN RRAM devices, XPS analysis was adopted to characterize the distribution of oxygen. The XPS data, which were obtained at a fixed sputtering rate, shows localization near the interface. Figures 3a and 3b show the XPS spectra of the Hf 4f core levels of the pure HfO_2 thin film and the Hf/HfO_2 structure. Figure 3a shows that the Hf 4f core level correlates with the pure HfO_2 thin film. However, the Hf 4f region in the Hf/HfO_2 structure correlates with three spin-orbit doublets, each with corresponding $4f_{7/2}$ binding energies at 14.21, 15.4, and 18.26 eV.[22] The pink, green and red lines in this figure represent the Hf metal (Hf^o), the suboxide (HfO_x) and the fully oxidized hafnium (HfO_2) signals,

respectively. These XPS results confirm the presence of an interfacial layer between the Hf metal and the HfO_2 thin film. Based on these results, the Pt/Hf/HfO_2/TiN RRAM device with an interfacial layer between the Hf layer and the HfO_2 thin film was dominated by the SCLC conduction mechanism. The polarity reversion of resistive switching behaviors can be explained by the effect of the interfacial layer, which fixes the oxygen diffusion region in the upper interface. The Pt/HfO_2/TiN devices did not exhibit this phenomenon. Figure 4 shows the possible switching mechanism with different directions of applied bias. In virgin Pt/Hf/HfO_2/TiN devices after PMA (Fig. 4a), the oxygen storage layer getters oxygen ions and leaves charged oxygen vacancies in the oxide thin film, which makes the oxide thin film oxygen-deficient and conductive. Because the HfO_2 thin film becomes more conductive, a smaller-forming voltage (~1 V) can be applied to connect filaments formed by oxygen vacancies. When applying a positive bias to the top electrode (Fig. 4b), the external voltage enforces charged oxygen vacancies to form a conductive filament. This subsequently switches the device to the LRS. After applying a negative bias to the top electrode (Fig. 4c), the oxygen ions drift to the HfO_2 thin film from the interfacial layer and reoxidize the conductive filament, rupturing the filaments. This subsequently switches the device to the HRS. Figures 5a and 5b show a comparison of the uniformity parameters of the two devices based on cumulative probability statistics. The Pt/Hf/HfO_2/TiN RRAM devices exhibit more uniform resistive switching performance than Pt/HfO_2/TiN RRAM devices in both resistance and voltage distributions. The low operation voltages (lower than 1 V) in the Pt/Hf/HfO_2/TiN device, reveals the potential for low-power RRAM applications. The Pt/Hf/HfO_2/TiN devices also exhibit excellent resistive switching properties in both the endurance and retention test. After a 10^3 dc sweep, the HRS and LRS

maintain a stable resistance ratio higher than ten without decay, as shown in Fig. 6a. The dispersion of operation voltages demonstrates the high switching uniformity, as shown in Fig. 6b. Figure 6c shows their good data storage ability (3×10^4 s) under 100 mV stress at 85 ^{o}C with nondestructive read-out.

4. Conclusion

In conclusion, this study shows that inserting a Hf metal layer into a Pt/HfO_2/TiN device and subjecting it to a PMA process creates a Pt/Hf/HfO_2/TiN device that exhibits polarity reversion in the resistive switching property. Inserting a Hf metal layer and performing the PMA process activated the Hf metal layer as an oxygen storage layer, which makes redox fixed near the interface between the Hf metal and the HfO_2 thin film. Consequently, the interface generation (HfO_x) that makes the conduction mechanism switch to SCLC mechanism from Poole-Frenkel emission, leading to a polarity reversion. The proposed Pt/Hf/HfO_2/TiN devices also exhibited good resistive switching characteristics and switching uniformity, with a low-voltage operation, 10^3 dc sweep endurance, and 3×10^4 s retention test at 85 ^{o}C.

Acknowledgments

The authors would like to express heartfelt thanks to the Prof. S.-J. Lin and the late Prof. T.-B. Wu from National Tsing-Hua University. C.-S. Peng is grateful to Dr. D.-T. Lee and G.H. Group for their helpful discussions. We also appreciate the Industrial Technology Research Institute of Taiwan (under Contract A351AA5110) and National Science Council of Taiwan (under Contract NSC 101-2120-M-007-003) for providing financial support.

References and Notes

1. I.G. Baek, M. S. Lee, S. Seo, M. J. Lee, D. H. Seo, D.-S. Suh, J. C. Park, S.O. Park, H. S. Kim, I. K. Yoo, U-In Chung, and J. T. Moon, *Tech. Dig.- Int. Electron Devices Meet*. 587 **(2004)**.

2. H.-Y. Lee, Y.-S. Chen, P.-S. Chen, P.-Y. Gu, Y.-Y. Hsu, S.-M. Wang, W.-H. Liu, C.-H. Tsai, S.-S. Sheu, P.-C. Chiang, W.-P. Lin, C.-H. Lin, W.-S. Chen, F.-T. Chen, C.-H. Lien, and M.-J. Tsai, *Tech. Dig.- Int. Electron Devices Meet*. 460 **(2010)**.

3. J.-J. Huang, Y.-M. Tseng, C.-W. Hsu, and T.-H. Hou, *IEEE Electron Device Lett.* 32, 1427 **(2011)**.

4. L. Kang, K. Onishi, Y. Jeon, B. H. Lee, C. Kang, W.-J. Qi, R. Nieh, S. Gopalan, R. Choi, and J. C. Lee, *Tech. Dig.- Int. Electron Devices Meet.* 35 **(2000)**.

5. W.-Y. Chang, K.-J. Cheng, J.-M. Tsai, H.-J. Chen, F. Chen, M.-J. Tsai, and T.-B. Wu, *Appl. Phys. Lett.* 95, 042104 **(2009)**.

6. H. Zhang, L. Liu, B. Gao, Y. Qiu, X. Liu, J. Lu, R. Han, J. Kang, and B. Yu, *Appl. Phys. Lett.* 98, 042105 **(2011)**.

7. C.-S. Peng, W.-Y. Chang, Y.-H. Lee, M.-H. Lin, F. Chen, M.-J. Tsai, *Electrochem. Solid-State Lett.* 15, H88 **(2012)**.

8. B. Govoreanu, G. S. Kar, Y-Y. Chen, V. Paraschiv, S. Kubicek, A. Fantini, I. P. Radu, L. Goux, S. Clima, R. Degraeve, N. Jossart, O. Richard, T. Vandeweyer,

K. Seo, P. Hendrickx, G. Pourtois, H. Bender, L. Altimime, D. J. Wouters, J. A. Kittl, M. Jurczak, *Tech. Dig.- Int. Electron Devices Meet.* 729, **(2011)**.

9. D.-Y. Lee, T.-Y. Tseng, *J. Appl. Phys.*, 110, 114117 **(2011)**.
10. H.-Y. Lee, Y.-S. Chen, P.-S. Chen, T.-Y. Wu, F. Chen, C.-C. Wang, P.-J. Tzeng, M.-J. Tsai, and C. Lien, *IEEE Electron Device Lett.* 31, 44 **(2010)**.
11. W.-Y. Chang, H.-W. Huang, W.-T. Wang, C.-H. Hou, Y.-L. Chueh, and J.-H. He, *J. Electrochem. Soc.* 159, G29 **(2012)**.
12. H. K. Yoo, S. B. Lee, J. S. Lee, S. H. Chang, M. J. Yoon, Y. S. Kim, B. S. Kang, M.-J. Lee, C. J. Kim, B. Kahng, and T. W. Noh, *Appl. Phys. Lett.* 98, 183507 **(2011)**.
13. S. Yu, X. Guan, and H.-S. Philip Wong, *Appl. Phys. Lett.* 99, 063507 **(2011)**.
14. Z. Wang, W. G. Zhu, A. Y. Du, L. Wu, Z. Fang, X. A. Tran, W. J. Liu, K. L. Zhang, and H.-Y. Yu, *IEEE Trans. Electron Devices* 59, 1203 **(2012)**.
15. W. J. Zhu, T.-P. Ma, T. Tamagawa, J. Kim, and Y. Di, *IEEE Electron Device Lett.* 23, 97 **(2002)**.
16. H. Wang, Y. Wang, J. Zhang, C. Ye, H. B. Wang, J. Feng, B. Y. Wang, Q. Li, and Y. Jiang, *Appl. Phys. Lett.* 93, 202904 **(2008)**.
17. J. R. Yeargan, H. L. Taylor, *J. Appl. Phys.* 39, 5600, **(1968)**
18. W. R. Harrell, J. Frey, *Thin Solid Films* 352, 195 **(1999)**.

19. K. Kukli, M. Ritala, T. Sajavaara, J. Keinonen, and M. Leskelä, *Chem. Vap. Deposition* 8, 199 (**2002**).

20. X. Liu, S. Ramanathan, A. Longdergan, A. Srivastava, E. Lee, T. E. Seidel, J. T. Barton, D. Pang, and R. G. Gordon, *J. Electrochem. Soc.* 152, G213 (**2005**).

21. T. Harada, I. Ohkubo, K. Tsubouchi, H. Kumigashira, T. Ohnishi, M. Lippmaa, Y. Matsumoto, H. Koinuma, and M. Oshima, *Appl. Phys. Lett.* 92, 222113 (**2008**).

22. S. Suzer, S. Sayan, M. M. Banaszak Holl, E. Garfunkel, Z. Hussain, and N. M. Hamdan, *J. Vac. Sci. Technol. A* 21**,** 106 (**2003**).

Figure captions

Figure 1. Reverse polarity operation in resistive switching between Pt/HfO_2/TiN and Pt/Hf/HfO_2/TiN devices.

Figure 2. Curve fitting in Pt/HfO_2/TiN devices (a) Poole-Frenkel emission and in Pt/Hf/HfO_2/TiN devices (b) SCLC mechanism.

Figure 3. XPS spectra of Hf 4f core levels : (a) the HfO_2 thin film. (b) interface between Hf/HfO_2.

Figure 4. Possible scenarios of switching mechanisms for the Pt/Hf/HfO_2/TiN device with positive-bias or negative-bias voltage.

Figure 5. Statistical distribution of resistive switching parameters during 100 continuous cycles in both Pt/HfO_2/TiN and Pt/Hf/HfO_2/TiN devices. (a) HRS and LRS. (b) V_{set} and V_{reset} .

Figure 6. The 10^3 stable endurance cycles of the Pt/Hf/HfO_2/TiN device: (a) HRS and LRS, (b) V_{set} and V_{reset} . (c) Data retention characteristics at 85 ^oC under 100mV stress.

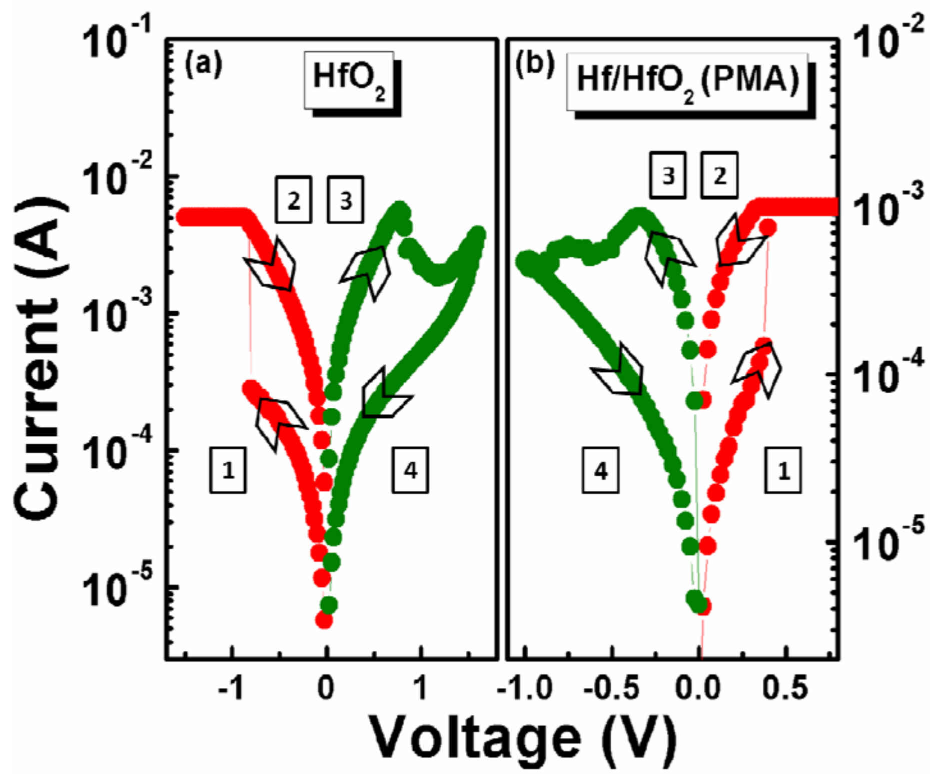

Figure 1. Peng et al.

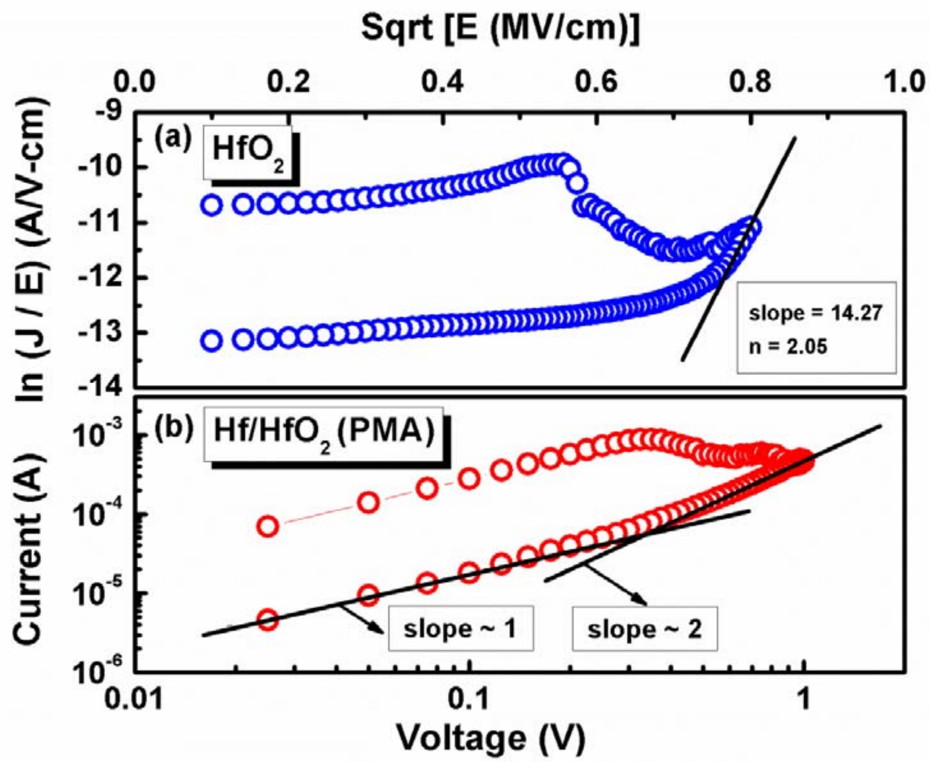

Figure 2. Peng et al.

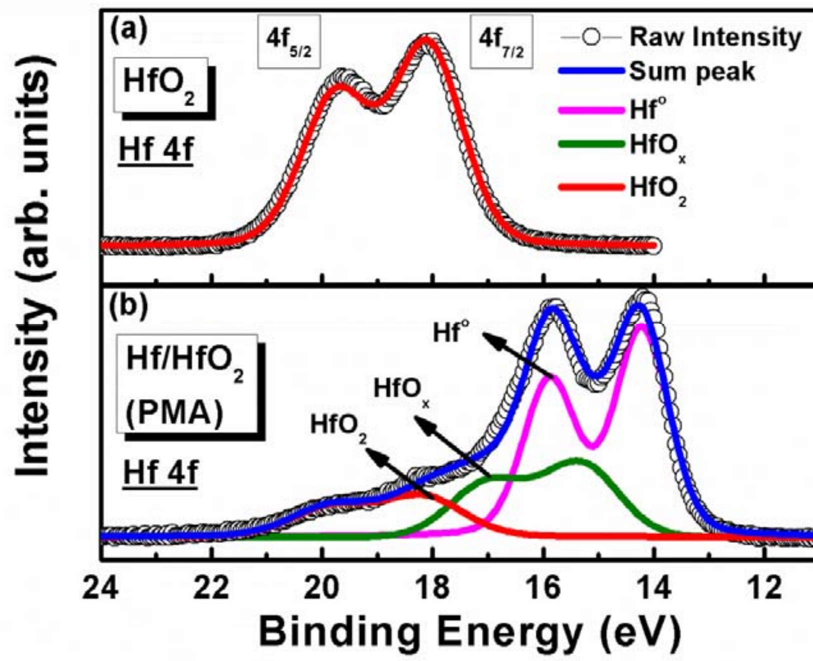

Figure 3. Peng et al.

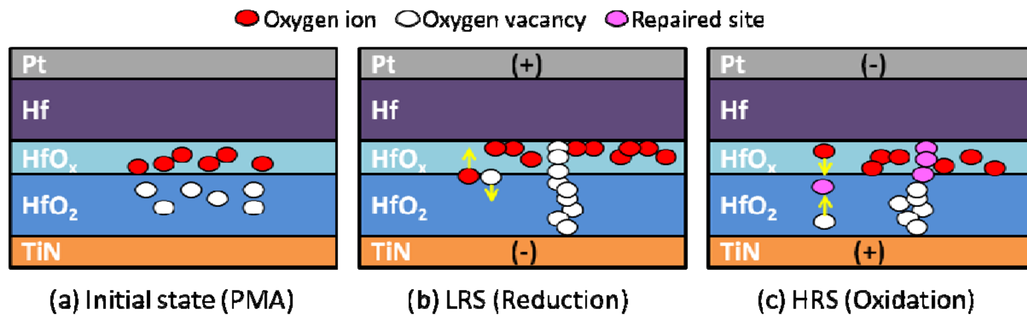

Figure 4. Peng et al.

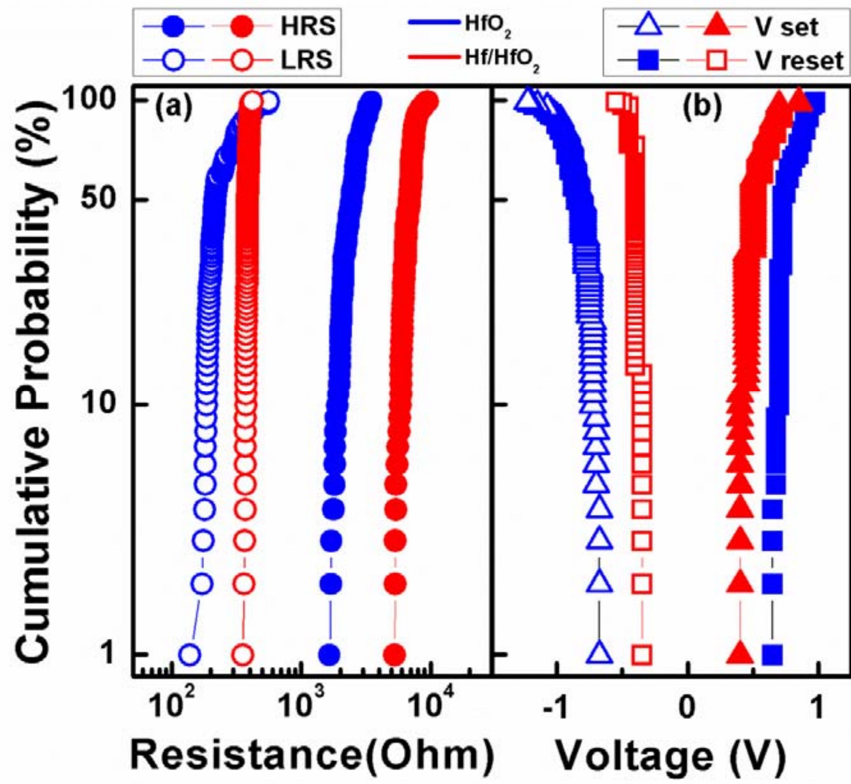

Figure 5. Peng et al.

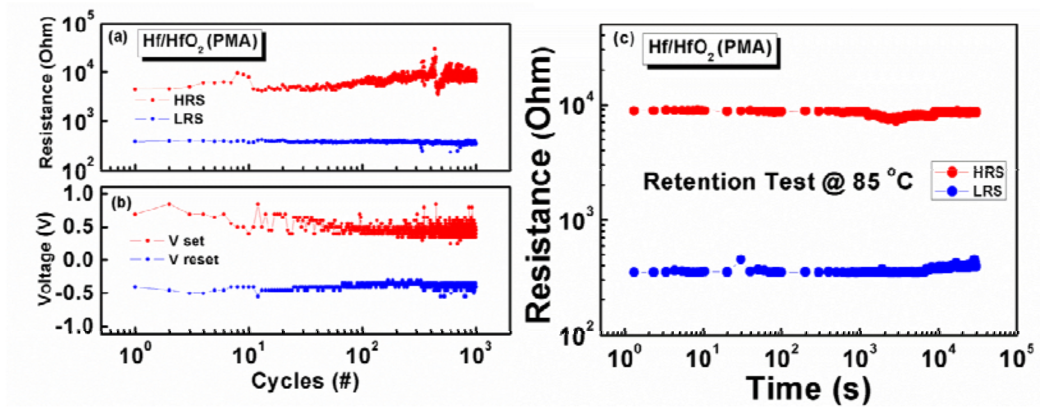

Figure 6. Peng et al